Biomaterials 30 (2009) 2967–2974

Contents lists available at ScienceDirect

Biomaterials

journal homepage: www.elsevier.com/locate/biomaterials

Leading Opinion

X-ray microcomputed tomography for the measurement of cell adhesion and proliferation in polymer scaffolds☆

Shauna M. Dorsey, Sheng Lin-Gibson, Carl G. Simon, Jr.*

Polymers Division, National Institute of Standards & Technology, 100 Bureau Drive, Gaithersburg, MD 20899, USA

ARTICLE INFO

Article history:
Received 20 January 2009
Accepted 23 February 2009
Available online 14 March 2009

Keywords:
3D imaging
Cell adhesion
Cell proliferation
Polymer scaffold
Salt-leaching
X-ray microcomputed tomography

ABSTRACT

We have explored the use of X-ray microcomputed tomography (μCT) for assessing cell adhesion and proliferation in polymer scaffolds. Common methods for examining cells in scaffolds include fluorescence microscopy and soluble assays for cell components such as enzymes, protein or DNA. Fluorescence microscopy is generally qualitative and cannot visualize the scaffold interior. Soluble assays quantitatively measure cell number but do not yield information on cell spatial distribution. Herein, the ability of μCT to detect cells in scaffolds was compared with fluorescence microscopy and a soluble DNA assay. Comparisons were performed using polymer scaffolds that were seeded with cells at different densities and cultured for different times. The results showed that fluorescence microscopy had better resolution than μCT and that the soluble DNA assay was approximately 5× more sensitive than μCT under the conditions tested. However, μCT was able to image through opaque scaffolds to yield quantitative 3D imaging and analysis via a single, non-invasive modality. Quantitative μCT analysis of cell penetration into scaffolds was demonstrated. Further, quantitative μCT volume analysis required that the cell density in the scaffolds be greater than 1 million cells per mL indicating that μCT is best suited for quantifying cells at relatively high density during culture in scaffolds. In sum, the results demonstrate the benefits and limitations of using μCT for 3D imaging and analysis of cell adhesion and proliferation in polymer scaffolds.

Published by Elsevier Ltd.

1. Introduction

We have investigated the ability of X-ray microcomputed tomography (μCT) to make quantitative, three-dimensional (3D) measurements of cell adhesion and proliferation in polymeric tissue engineering scaffolds. The use of degradable polymer scaffolds to facilitate organ and tissue regeneration constitutes one of the basic tenets in the field of tissue engineering [1,2]. Thus, tools to image and quantify tissue generation in scaffolds are useful and desirable. It is especially important to be able to see inside the scaffolds to measure tissue generation on the scaffold interior.

The most common method for examining cells in scaffolds is microscopy [1,3–6]. Sectioning followed by histology can image the scaffold interior but is destructive, tedious and only semi-quantitative [1,3]. Fluorescence microscopy can be quantitative when high-throughput approaches are applied [7,8] and confocal fluorescence microscopy can yield 3D images [4–6]. However, neither can "see through" opaque materials to image the interior of a scaffold. Other common methods for measuring cell presence include the colorimetric and fluorometric soluble assays for enzymes (dehydrogenase) [9–11], protein (BCA) [12,13] or DNA (Picogreen) [14,15]. These soluble assays are quantitative but do not yield information on cell distribution. In contrast, μCT generates 3D images, can penetrate deep into the scaffold interior, is non-destructive and is inherently quantitative [16–20]. For these reasons, we have investigated the sensitivity of using μCT to image and measure cell adhesion and proliferation in polymeric tissue engineering scaffolds.

In order to test the ability of μCT to assess cell adhesion and proliferation in polymer scaffolds, cells were seeded onto polymer scaffolds at six different concentrations and measured at different time points. Poly(ε-caprolactone) (PCL) was chosen as the material for scaffold fabrication because it is biocompatible and has been cleared by FDA for use in biomedical implants [21,22]. A salt-leaching approach was chosen because it is a common and effective

☆ *Editor's Note*: This paper is one of a newly instituted series of scientific articles that provide evidence-based scientific opinions on topical and important issues in biomaterials science. They have some features of an invited editorial but are based on scientific facts, and some features of a review paper, without attempting to be comprehensive. These papers have been commissioned by the Editor-in-Chief and reviewed for factual, scientific content by referees.

* Corresponding author. Tel.: +1 301 975 8574; fax: +1 301 975 4977.
E-mail address: carl.simon@nist.gov (C.G. Simon Jr.).

0142-9612/$ – see front matter Published by Elsevier Ltd.
doi:10.1016/j.biomaterials.2009.02.032

method for scaffold fabrication [1,5]. The MC3T3-E1 osteoblast cell line was used because it is a well-characterized murine osteoblast model which has been widely applied for regenerative orthopaedic applications [3,5,11,23]. Cell adhesion and proliferation after 1 d, 7 d or 14 d of culture on the scaffolds were assessed by three techniques: fluorescence microscopy, a soluble assay for DNA (Picogreen) and μCT. Results from the three approaches were compared so that the usefulness of μCT for detecting cells in tissue engineering scaffolds could be evaluated.

2. Materials and methods

2.1. Fabrication of polymer scaffolds

Polymer scaffolds were fabricated in poly(propylene) 96-well plates (Sigma) using a 10% mass per volume solution of PCL ($M_n = 80\,000$; Sigma) in dioxane [24]. NaCl (0.12 g) sieved to 0.250 mm–0.425 mm was placed in each well of the 96-well plate. A syringe pump was used to dispense 30 μL (2 drops) of PCL solution into each well. The wet 96-well plates were centrifuged to force the wetting of NaCl by PCL solutions [2 min, lid was on plates, 2000 rpm (210 rad/s), swinging bucket centrifuge]. The plates were frozen in liquid nitrogen, freeze-dried overnight (100 m Torr), salt-leached 5 d in water, air-dried 3 d and stored in a desiccator. Each 96-well PCL scaffold weighed 3 mg and approximately 300 scaffolds were fabricated for this manuscript.

2.2. Scanning electron microscopy

Scaffolds were frozen in liquid nitrogen and sectioned with a razor to expose interior. After sputter-coating with gold, internal scaffold structure was viewed by scanning electron microscopy (SEM, 15 kV, Hitachi S-4700-II FE-SEM).

2.3. Cell culture

The MC3T3-E1 murine osteoblast cell line (Riken Cell Bank) was cultured as described [7] in alpha-modification of Eagle's minimum essential medium (Cambrex Bio Science) supplemented with 10% volume fraction fetal bovine serum (Gibco) and 0.060 mg/mL kanamycin sulfate (Sigma). Medium was changed twice weekly and cultures were passaged with 2.5 g/L trypsin (0.25% mass fraction) containing 1 mmol/L EDTA (ethylenedinitrilotetraacetic acid; Gibco). A single passage 4 culture at 80% confluency was used for all experiments.

Scaffolds in 96-well plates were sterilized by ethylene oxide (Anderson Products) and degassed 2 d in a desiccator under vacuum. Medium (0.2 mL) was placed in each well and the plates were placed under vacuum for 2 min. The vacuum was released and re-applied 2 more times. Cycling of a vacuum wets the scaffolds with medium. Following trypsinization, cells were seeded onto scaffolds at varying densities in 0.2 mL of medium: (0, 5000, 10 000, 25 000, 100 000 or 400 000) cells per scaffold. Cells were cultured on the scaffolds in the 96-well plates for three different time points: 1 d, 7 d and 14 d (medium changed twice per week). Note that scaffolds seeded with 400 000 cells could only be cultured for 1 d because their medium became acidic at 7 d and 14 d due to the high level of cellular metabolism. Also note that a shorthand for the scaffolds is used where "100 K-1d" indicates a scaffold seeded with 100 000 cells and cultured for 1 d.

2.4. Fluorescence imaging

For fluorescence imaging, scaffolds were prepared in triplicate for each treatment requiring 54 scaffolds (6 seeding densities × 3 time points × 3 replicates). Cells on scaffolds were fixed for 5 min (0.5% mass fraction Triton X-100, 4% mass fraction paraformaldehyde, 5% mass fraction sucrose, 1 mmol/L $CaCl_2$, 2 mmol/L $MgCl_2$ in phosphate buffered saline, pH 7.4), post-fixed for 20 min (same as fix but without Triton X-100) and blocked for 1 h (1% mass fraction bovine serum albumin). Fixed cells were fluorescently stained for 1 h in phosphate buffered saline (PBS) containing 1 μmol/L Sytox green (Invitrogen). Stained scaffolds were removed from 96-well plates and put on a glass slide while moist with PBS for imaging. Cells on scaffolds were imaged with an inverted epifluorescence microscope using a 4× objective and digital images were captured.

2.5. Soluble DNA assay

For the soluble DNA assay, 6 replicate scaffolds were prepared for each treatment requiring a total of 108 scaffolds (6 seeding densities × 3 time points × 6 replicates). At the indicated time points (1 d, 7 d or 14 d), the medium was removed from the scaffolds in the 96-well plates and 0.2 mL of lysis buffer [0.2 mg/mL Proteinase K (19 Units/mg; Sigma) and 0.2 mg/mL sodium dodecyl sulfate (SDS; 0.02% mass per volume) in PBS] was added to each scaffold. The scaffolds were incubated 16 h at 37 °C with lysis buffer and then a 0.1 mL aliquot of the lysates was transferred to a clean polystyrene 96-well plate. The 0.1 mL aliquot was diluted 1:1 with a 200-fold dilution of the Picogreen reagent solution (Invitrogen) and a platereader was used to determine fluorescence intensity (excitation 485 nm; emission 538 nm). A DNA standard curve was prepared to calibrate readings.

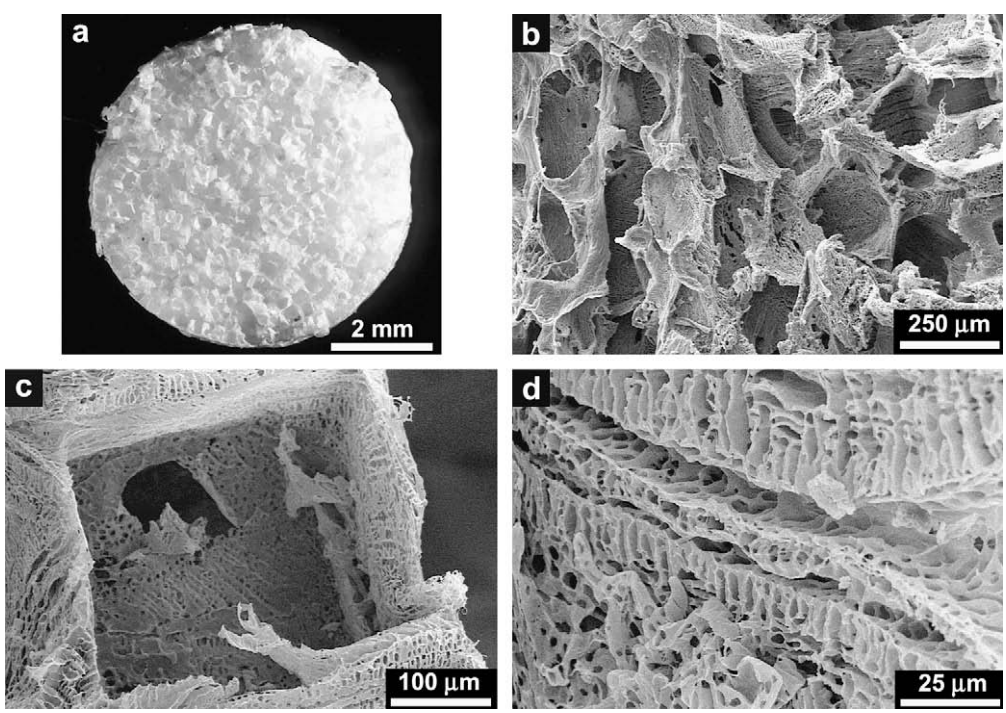

Fig. 1. (a) A PCL scaffold fabricated in a 96-well plate and imaged by a stereomicroscope is shown. Scanning electron micrographs of the interior of a PCL scaffold at low (b), medium (c) and high (d) magnification are shown. In (b) the large-scale pores (0.2 μm–0.4 mm) formed by salt-leaching are shown. In (c), a single cuboidal pore is shown that formed as a result of salt-leaching. In (d), small-scale pores (<10 μm) that form in the scaffold struts as a result of dioxane sublimation during freeze-drying are shown.

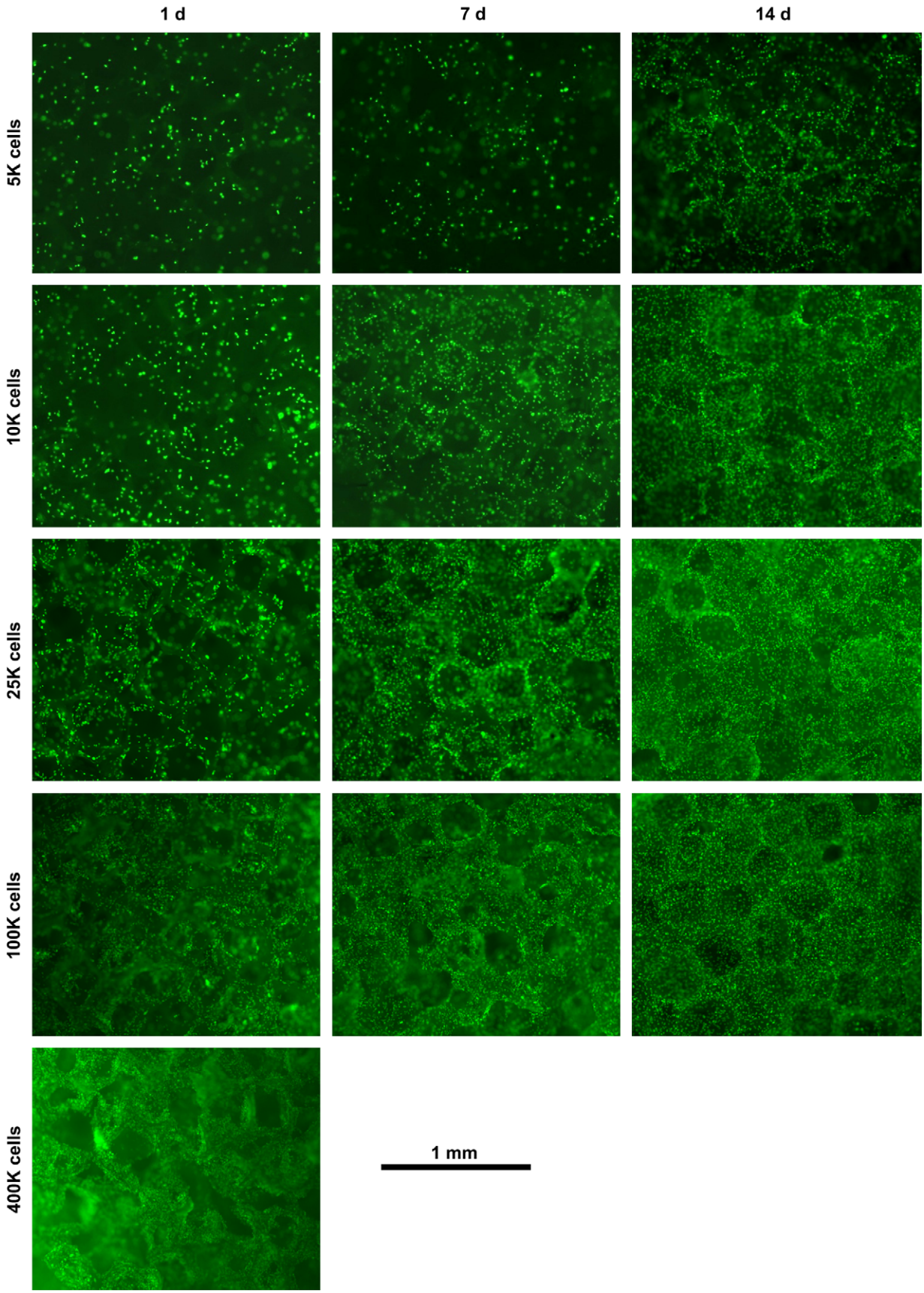

Fig. 2. MC3T3-E1 osteoblasts were seeded on PCL scaffolds at 6 different densities [(0, 5000, 10 000, 25 000, 100 000 or 400 000) cells per scaffold] and cultured for 3 different times (1 d, 7 d and 14 d). At the indicated times, cells were fixed, the nuclei were stained with Sytox green and cells were imaged by fluorescence microscopy using a 4× objective. The scale bar at the bottom of the figure applies to all panels. Green dots in the images are nuclei of cells adherent to scaffolds. Note how cells adherent to the scaffold struts make the large pores formed by salt-leaching (0.2 mm–0.4 mm) become apparent at the high seeding densities and longer culture times.

this should be support 2

2.6. X-ray microcomputed tomography

For imaging by μCT, 6 replicate scaffolds were prepared for each treatment requiring a total of 108 scaffolds (6 seeding densities × 3 time points × 6 replicates). At the indicated time points (1 d, 7 d or 14 d), the scaffolds were fixed overnight (1% mass fraction glutaraldehyde in PBS), washed with PBS, stained with osmium tetroxide (1% mass fraction OsO_4 in PBS) [17], washed with PBS, washed with water and air-dried for 3 d. Osmium is a heavy metal that stains cell membranes, scatters X-rays and makes cells visible by μCT. Stained and dried scaffolds were imaged by μCT [Scanco μCT 40, 55 kVp, 145 μA, 8 μm voxel size (slice thickness), 0.3 s integration, 325 slices, sigma 1.2, support 1.2, threshold 34]. Threshold 34 was used because at this value 95% of the voxels were attributable to osmium-stained cells (not scaffold or background). This was determined by comparing a voxel intensity histogram from a scaffold region rich in cell coverage with a histogram from a region containing little to no cells (see Section 3 for a more detailed explanation). The voxel intensities provided by the instrument are on a scale of −32767 to 32767. However, the thresholds that can be chosen to render a reconstruction range between 0 and 1000. Thus, the instrument voxel intensities were divided by 32.767 to put them on the same scale as threshold values (−1000 to 1000). Note that negative voxel intensity values represent instrument noise and are not physically meaningful.

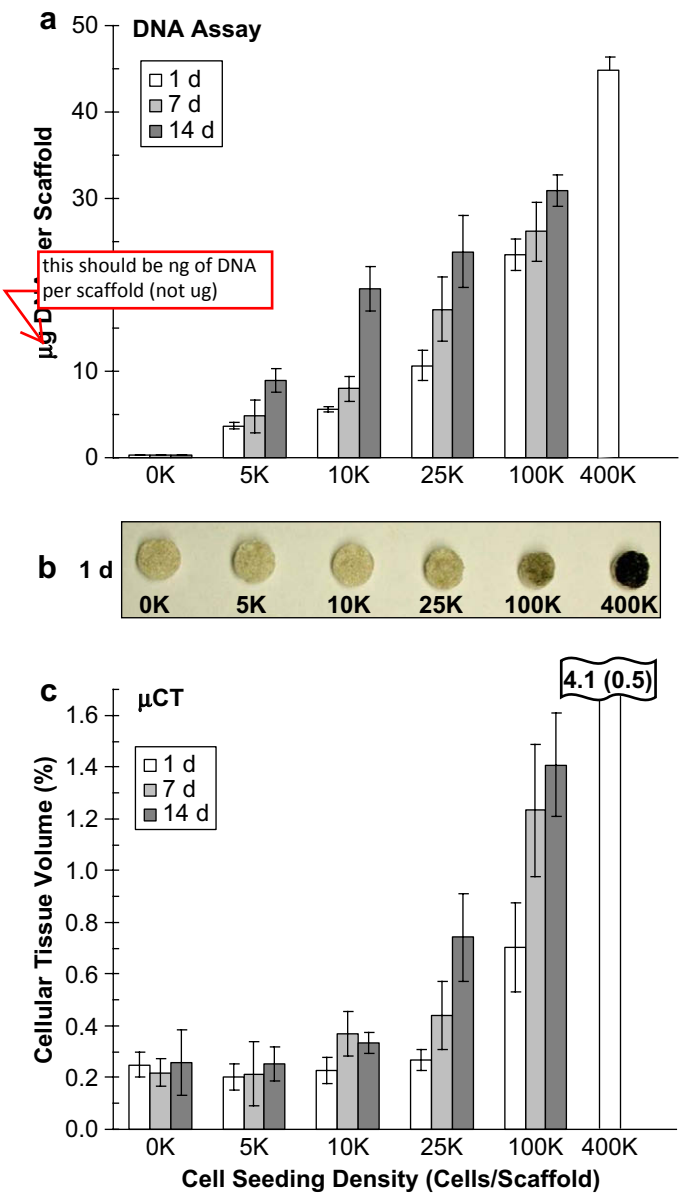

Fig. 3. MC3T3-E1 osteoblasts were seeded on PCL scaffolds at 6 different densities [(0, 5000, 10 000, 25 000, 100 000 or 400 000) cells per scaffold] and cultured for 3 different times (1 d, 7 d and 14 d). (a) DNA on the scaffolds was measured with a soluble DNA assay. Error bars are standard deviation ($n = 6$). ANOVA with Tukey's test for multiple comparisons indicated that all conditions were significantly different from background (0 K, scaffolds without cells) except "5K" at 1 d and at 7 d ($P < 0.05$). (b) A photograph of scaffolds that were seeded with the indicated number of cells, cultured 1 d and stained with osmium tetroxide is shown. Notice that the intensity of the black osmium staining on the scaffolds increases with increasing cell seeding density. (c) Cellular tissue volume on the scaffolds was determined from μCT images using a threshold of 34. Note that 95% of the voxels with intensity ≥34 were attributable to cellular tissue (not the scaffold). Error bars are standard deviation ($n = 6$). ANOVA with Tukey's test for multiple comparisons indicated that 25 K-14d, 100 K-1d, 100 K-7d, 100 K-14d and 400 K-1d were significantly different from background (0 K, scaffolds with no cells) ($P < 0.05$). Note that 400 K-1d goes off-scale so the average and standard deviation are given in a banner at the top of the bar.

3. Results and discussion

Cylindrical scaffolds (diameter = 6.5 mm, height ≈ 2.5 mm) were used for all experiments and one that was gently removed from a 96-well plate is shown in Fig. 1a. Large pores of size range 0.2 mm–0.4 mm resulting from NaCl leaching were observed in the scaffold interiors by SEM (Fig. 1b and c). Smaller voids (<10 μm) which formed during dioxane sublimation were observed in the scaffold walls (Fig. 1d). Un-dissolved NaCl crystals were not observed in the scaffolds by SEM indicating that all NaCl was leached and that pores were interconnected. Porosity was calculated from the PCL density (1.1 g/mL; Sigma–Aldrich), scaffold mass and scaffold volume as described previously [24]. The total porosity was approximately 97% where larger pores from NaCl leaching caused 83% porosity and "dioxane-sublimation voids" in the scaffold wall resulted in 14% porosity.

Cells were imaged by fluorescence microscopy and DNA measured by Picogreen for comparison to μCT. Fluorescence micrographs show that cell numbers increased with increasing cell seeding density and increasing culture time for all conditions tested indicating osteoblasts adhered and proliferated on the polymer scaffolds (Fig. 2). Similar results were obtained for the soluble DNA assay where increased DNA levels were extracted from the scaffolds with increasing cell seeding density and increasing culture time (Fig. 3a). Analysis of variance (ANOVA) with Tukey's test for multiple comparisons of the DNA data indicated that all conditions

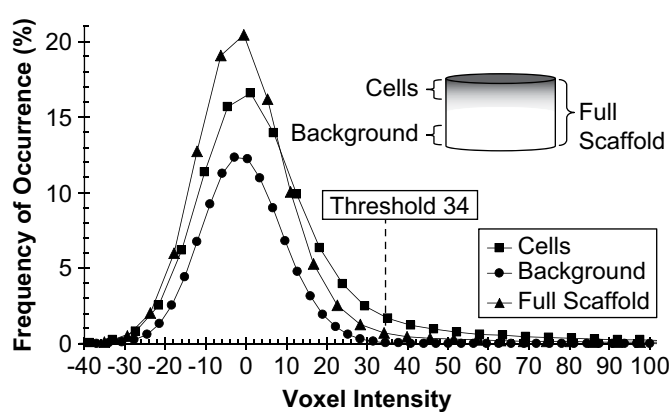

Fig. 4. Voxel intensity histograms from μCT scans of the osmium-stained scaffolds were used for threshold selection. The "Cells" histogram was generated from the top 100 slices (800 μm) of a 100 K-1d scaffold. Most of the cells seeded on the scaffolds resided in the top region of the scaffolds because the walls of the 96-well plates prevented the cells from accessing the bottom regions of the scaffolds. The "Background" histogram was generated from the bottom 100 slices (where there were few cells) of the same 100 K-1d scaffold. The ratio of the "areas under the histograms to the right of voxel intensity 34" for "Cells" to "Background" was 95:5 (95% of the signal was from cells and 5% was from background). 95% of the voxels with intensity ≥34 were due to osmium-stained cells and not to background (scaffold, noise, voids, etc.). Thus, a threshold of 34 was used for all μCT analyses. The "Full Scaffold" histogram was generated from all 325 slices of the 100 K-1d scaffold and is representative of the distribution of data used to calculate actual cell volumes given in Fig. 3c.

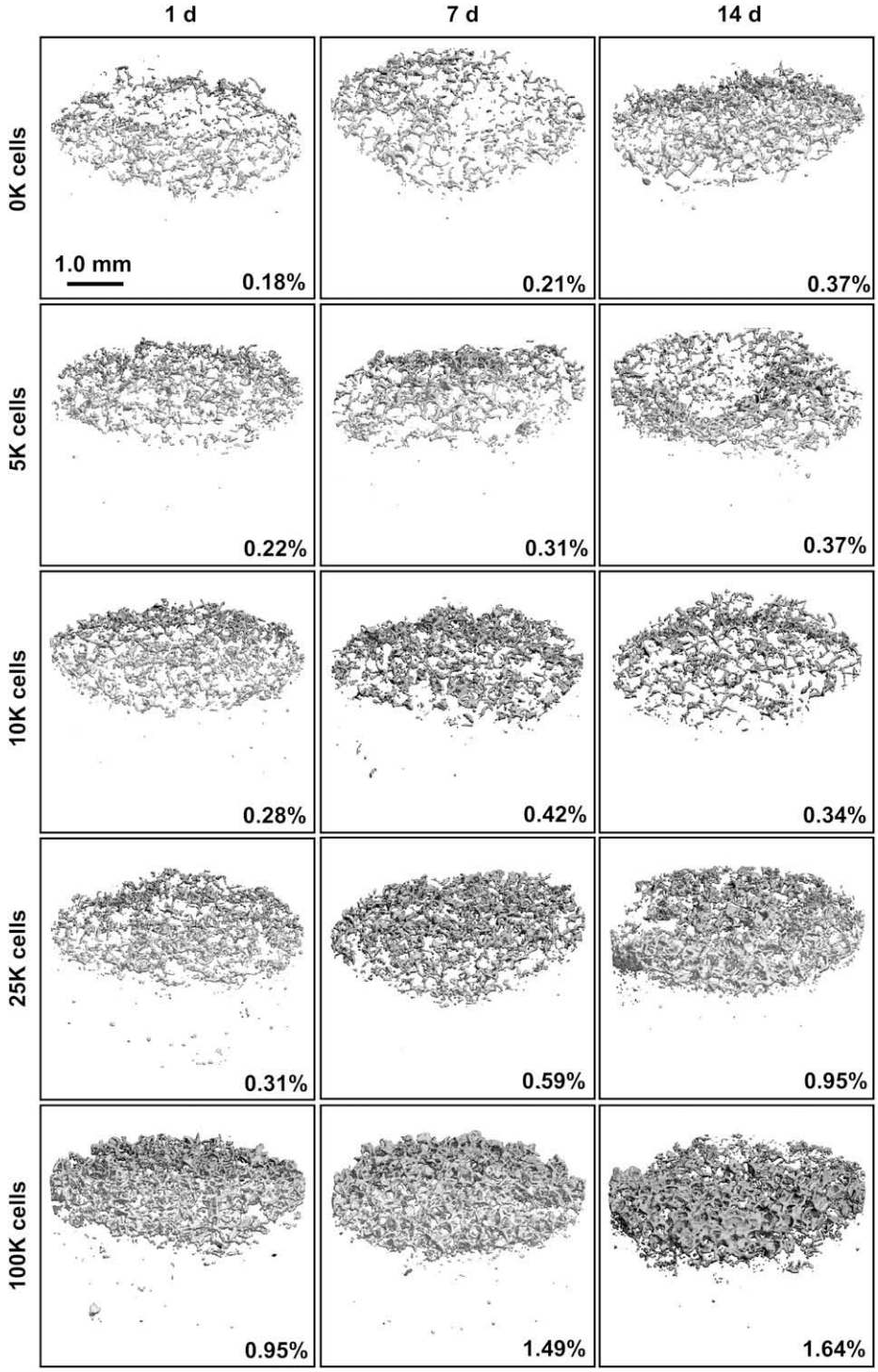

Fig. 5. μCT images of cells cultured on scaffolds for the cell seeding densities and culture times indicated in the figure are shown. The size bar in the upper left panel applies to all panels. The number in the bottom right of each panel indicates the percent of the scaffold volume that is occupied by cells. Note that the opaque voxels in the images are not from the scaffold but are from cells on the scaffold. The threshold for the images was set at 34, which is above the range where the scaffolds are visible.

were significantly different ($P < 0.05$) from the background (scaffolds without cells) except "5K" at 1 d and at 7 d. These data show that greater than 5000 cells must be seeded on a scaffold to enable quantitative detection of cell adhesion and proliferation under the conditions tested for the DNA assay.

For imaging by μCT, the cells on the scaffolds were stained with osmium tetroxide to enhance their X-ray contrast. The osmium staining of the cells on the scaffolds is visible with the naked eye as shown in Fig. 3b. Staining up to 25 000 cells looks the same as "0K", but the "100K" and "400K" are visibly darker. These results demonstrate that greater than 25 000 cells must be seeded on a scaffold in order to be visible by gross visual inspection.

The osmium-stained scaffolds were scanned by μCT and voxel intensity histograms were generated to enable selection of an appropriate threshold for 3D image analysis (Fig. 4). The histogram from a 100 K-1d scaffold ("Full Scaffold", all 325 slices) does not

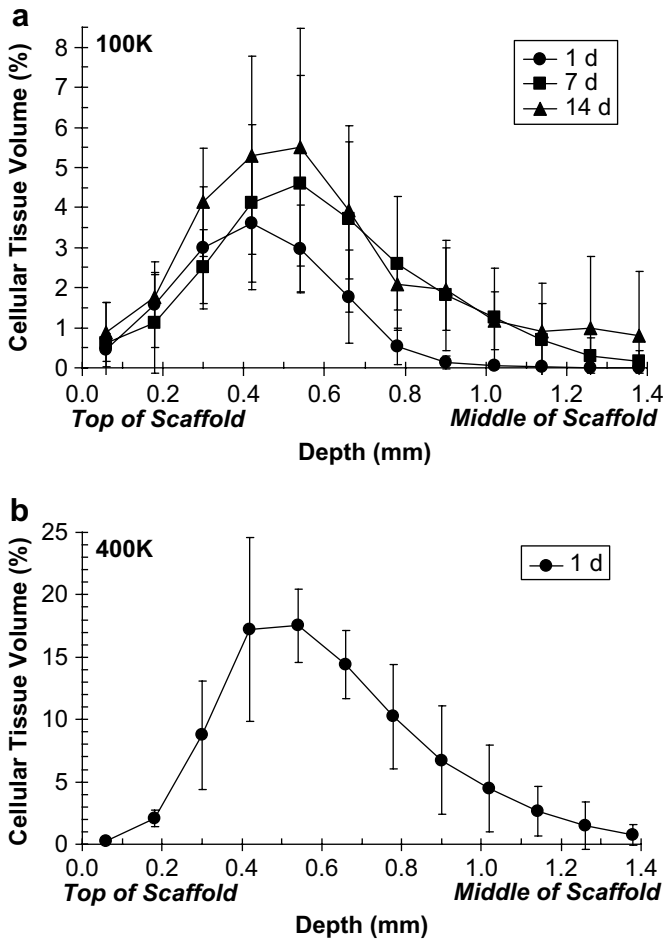

Fig. 6. Cell penetration depth into the scaffolds was evaluated by μCT image analysis. μCT scans of scaffolds were divided in the *Z*-direction into 12 regions of 15 slices (120 μm) for cellular tissue volume analysis (threshold 34). (a) Plots from scaffolds seeded with 100 000 cells and cultured 1 d, 7 d or 14 d. (b) Plots from scaffolds seeded with 400 000 cells and cultured 1 d. Error bars represent standard deviation ($n = 6$).

present a minimum between background (scaffold and voids constitute background) and the cellular tissue to use as threshold. Thus, the threshold we used was that at which 95% of the voxel intensity signal came from the cells (background accounts for the other 5%). To determine this optimum threshold, two additional histograms are generated in Fig. 4: one from a scaffold region rich in cell coverage ("Cells" histogram from the top 800 μm of the scaffolds) and one from a scaffold region containing no cells ("Background" histogram from bottom 800 μm of the scaffolds). Cells settled primarily on the top region of the scaffolds in the 96-well plate because the walls of the wells prevented cell access to scaffold bottoms. For the "Background" histogram, the frequency of occurrence approached 0 as the voxel intensity approached 35. In contrast, the "Cells" histogram shows appreciable signal up through voxel intensity 100. We calculated the areas under the histograms to the right of a range of voxel intensities (30–40) for the "Cells" histogram and the "Background" histogram and then determined the ratio of the areas (Fig. 4). Calculations carried out for the 6 "100 K-1d" scaffolds identified 34 (standard deviation = 4) as the optimum threshold. In other words, the ratio of the "area under the curve to the right of 34 for the Cells histogram" to the "area under the curve to the right of 34 for the Background histogram" was 95:5. Hence, a threshold of 34 was used for all μCT analyses.

Cell adhesion and proliferation during culture on scaffolds were determined by calculating the "percent tissue volume" in the μCT scans which is the percent of the voxels in a given scaffold volume that contained enough osmium-stained cellular material (tissue) to give that voxel an intensity value greater than 34. The full 325 slices of each scaffold were used to compute percent tissue volume. Results showed a trend of increased cell number with increasing cell seeding density and increasing culture time (Fig. 3c). ANOVA with Tukey's test for multiple comparisons showed that the "5K" and "10K" samples were not significantly different from background ($P > 0.05$). For "25K", the 1 d and 7 d specimens were not significantly different from background, but the 14 d specimen was ($P < 0.05$). Lastly, all of the "100K" and "400K" specimens were significantly different from background ($P < 0.05$). These results indicate that greater than 25 000 cells must be seeded onto a 96-well scaffold to enable detection by μCT and that μCT can quantify cell adhesion and proliferation in polymer scaffolds.

The corresponding μCT images are shown in Fig. 5 to display the spatial distributions of the cells in the scaffolds. Similar to the volume calculations in Fig. 3c, the cell density on the 5 K and 10 K scaffolds does not appear different from control scaffolds. For the 25 K and 100 K scaffolds, there is a visible increase in cell density and cell penetration depth into the scaffolds with increased culture time. The even X-ray contrast across the top of the 100 K-1d scaffolds indicates uniform cell adhesion radially and laterally on the scaffolds. The proliferation also appears to have occurred in an even manner radially and laterally across the scaffolds at 7 d and 14 d.

Cell penetration depth into the scaffolds was evaluated quantitatively by μCT image analysis. Scaffolds were divided in the *Z*-direction into 12 × 120 μm-thick regions (15 slices) for cellular tissue volume analysis (Fig. 6). For the 100 K scaffolds (Fig. 6a), the cells penetrated the scaffolds to a depth of 800 μm after 1 d. By 7 d, the cells had migrated an additional 400 μm into the scaffolds to a depth of 1200 μm. From 7 d to 14 d, the cells did not penetrate any further. Cell migration deeper into the scaffolds was probably prohibited by insufficient exchange of nutrients and waste since scaffolds in the 96-well plate format only have access to medium from their top surface. For the 400 K-1d scaffolds (Fig. 6b), cells penetrated to 1200 μm, however, 7 d and 14 d time points were unavailable due to acidic medium (well volume of only 0.2 mL was not sufficient to sustain 400 K cells). These results demonstrate the ability of μCT to generate 3D images of cellular tissue distribution that can be quantitatively analyzed to provide information about cell performance during culture in polymer scaffolds.

A higher magnification μCT image of a 400 K-1d scaffold is shown in Fig. 7a. Note that the 3D contours of the salt-leached pores in the scaffold are visible due to the confluent coating of osmium-stained osteoblasts that has adhered to them. The μCT (8 μm resolution) cannot resolve individual cells and can only resolve cell clusters (tissue, regions of confluent cells). A side by side comparison of a fluorescence micrograph and a μCT image at the same magnification (Fig. 7b and c) demonstrates the higher resolution afforded by fluorescence microscopy. Individual nuclei of osteoblasts adhering to the scaffold are visible in the fluorescence micrograph (Fig. 7b), while cells in the μCT image run together appearing as a pixelated, continuum on the scaffold (Fig. 7c). On the other hand, the μCT image more clearly portrays the 3D nature of cells being cultured on a scaffold and enables imaging through the opaque scaffold.

The comparison of the DNA assay with μCT in Fig. 3 indicates that the DNA assay was ≈5× more sensitive than μCT. The statistical analysis of the DNA assay showed that greater than 5000 cells had to be seeded on a scaffold to enable detection of above background (Fig. 3a). For the μCT volume analysis, greater than 25 000 cells had to be seeded on a scaffold to enable detection of signal

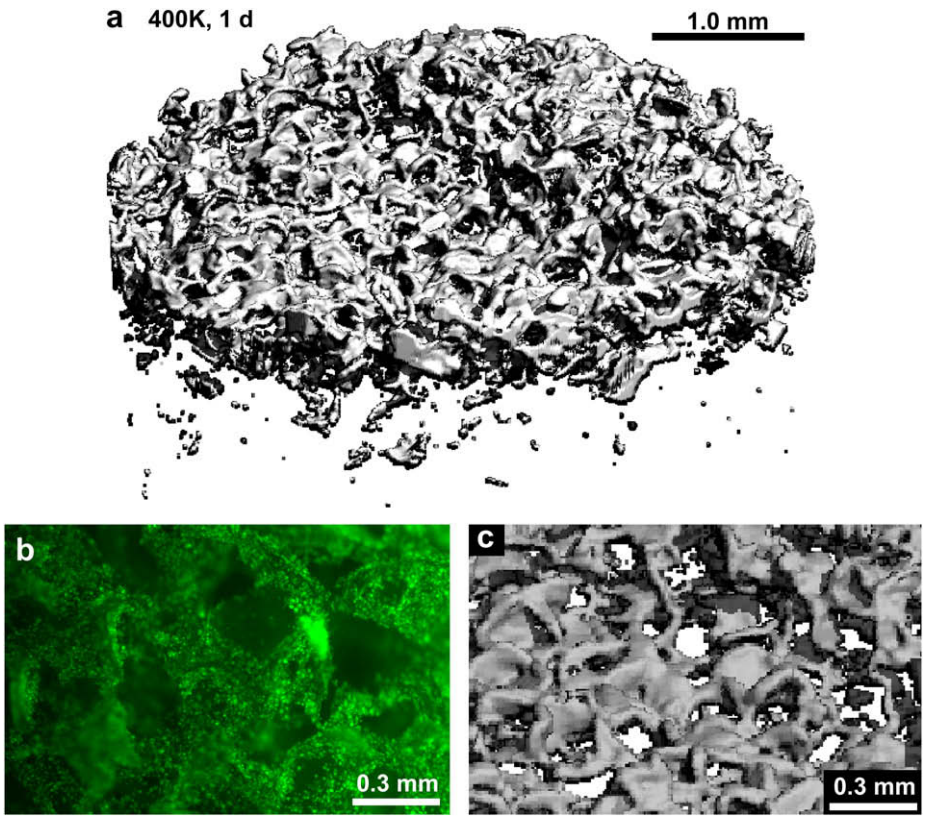

Fig. 7. (a) μCT image of a scaffold cultured 1 d with 400 000 cells (threshold 34; calculated cell volume is 3.95%). Side by side comparison of a (b) fluorescence micrograph and a (c) μCT image (threshold 34) from scaffolds cultured 1 d with 400 000 cells. Note that panels (b) and (c) are at the exact same magnification allowing direct comparison of the fluorescence and μCT images. The green dots in (b) are fluorescently stained nuclei of cells adherent to scaffolds. The grey contours in (c) represent confluent cell layers (not scaffold).

above background (Fig. 3c). These results indicate that μCT is best suited for situations where a high density of cells is present on a scaffold, such as in more mature constructs where cells have reached confluence and where tissue generation has begun.

The penetration depth data for the 100 K-1d scaffold in Fig. 6a indicates that after 1 d of culture the cells were present in the top 800 μm of the scaffolds. If it is assumed that there are 100 000 cells present in these scaffolds, then a volume calculation indicates that the cell density in the scaffolds during the μCT imaging was approximately 4×10^6 cells/mL {cells per unit volume = cell number/$(\pi r^2 \times h) = 100\,000$ cells/$[3.14 \times (0.325\ \text{cm})^2 \times 0.08\ \text{cm}] = 3.77 \times 10^6$ cells/mL}. Note that this calculation is approximate because it assumes that all the cells adhered, viability was 100%, the cells did not proliferate and the cells were evenly distributed across the scaffold (not patchy).

The μCT volume analysis in Fig. 3c demonstrated that the 100 K-1d scaffolds were easily distinguished from background, which indicates that a cell density of 4 million cells per mL is well within the detection limits of the μCT approach. A similar calculation for the 25 K-1d specimens indicates that cell density was roughly 1 million cells per mL for these scaffolds, which was a density that was not significantly different from background in the μCT volume analyses (Fig. 3c). Taken together, these results indicate that an approximate cell density of between 1 million and 4 million cells per mL is required for quantitative μCT volume analysis of cell adhesion and proliferation in polymer scaffolds.

4. Conclusions

The advantages and disadvantages of using μCT to quantify cell adhesion and proliferation in polymer scaffolds have been evaluated. Fluorescence microscopy had better imaging resolution than μCT and the soluble Picogreen DNA assay was more sensitive for cell quantification than μCT. However, μCT combined imaging and quantification into a single modality. μCT is inherently quantitative, can image through opaque scaffolding materials and yields 3D images which can be used to assess spatial distribution of cells in scaffolds. μCT required cell densities of greater than 1 million cells per mL indicating that this approach will work best for constructs that contain a high density of cells.

The three approaches for assessing cells in scaffolds addressed herein, fluorescence microscopy, soluble DNA assay and μCT, are complimentary to one another. When evaluating cell adhesion and proliferation in polymer scaffolds, use of florescence microscopy is essential for establishing that cells are present and that they are evenly distributed about the scaffold, especially at early time points when μCT cannot detect cells at low density. In addition fluorescence microscopy has higher resolution enabling individual cells to be visualized. The soluble DNA assay is valuable because it is quantitative and provides a second measure of cell number. Finally, μCT provides both a 3D image and 3D quantitative analysis of cell spatial distribution within scaffolds. In sum, μCT compliments fluorescence microscopy and soluble assays for cell components (DNA, protein, enzymes) to provide a comprehensive evaluation of cell adhesion and proliferation in polymeric tissue scaffolds.

Acknowledgements

We acknowledge valuable contributions from Jirun Sun, Nancy Lin, Diana Zeiger, Yanyin Yang (all from NIST) and Morgan

Alexander (University of Nottingham). S.M.D. acknowledges support from the NIST-NSF summer undergraduate research fellowship (SURF). This work was supported by NIST and by NIH/NIBIB R21 EB006497-01. Standard deviation (S.D.) is the same as the combined standard uncertainty for the purposes of this work. The content is solely the responsibility of the authors and does not necessarily represent the official views of the NIH, NIBIB or NIST. This article, a contribution of NIST, is not subject to U.S. copyright. Certain equipment and instruments or materials are identified in the paper to adequately specify the experimental details. Such identification does not imply recommendation by NIST, nor does it imply the materials are necessarily the best available for the purpose.

References

[1] Vacanti JP, Morse MA, Saltzman WM, Domb AJ, Perez-Atayde A, Langer R. Selective cell transplantation using bioabsorbable artificial polymers as matrices. J Pediatr Surg 1988;23(1 Pt 2):3–9.
[2] Langer R, Vacanti JP. Tissue engineering. Science 1993;260(5110):920–6.
[3] Shea LD, Wang D, Franceschi RT, Mooney DJ. Engineered bone development from a pre-osteoblast cell line on three-dimensional scaffolds. Tissue Eng 2000;6(6):605–17.
[4] Liu E, Treiser MD, Johnson PA, Patel P, Rege A, Kohn J, et al. Quantitative biorelevant profiling of material microstructure within 3D porous scaffolds via multiphoton fluorescence microscopy. J Biomed Mater Res Part B Appl Biomater 2007;82B(2):284–97.
[5] Dadsetan M, Hefferan TE, Szatkowski JP, Mishra PK, Macura SI, Lu L, et al. Effect of hydrogel porosity on marrow stromal cell phenotypic expression. Biomaterials 2008;29(14):2193–202.
[6] Yang Y, Dorsey SM, Becker ML, Lin-Gibson S, Schumacher GE, Flaim GM, et al. X-ray imaging optimization of 3D tissue engineering scaffolds via combinatorial fabrication methods. Biomaterials 2008;29(12):1901–11.
[7] Simon Jr CG, Eidelman N, Kennedy SB, Sehgal A, Khatri CA, Washburn NR. Combinatorial screening of cell proliferation on poly(L-lactic acid)/poly (D,L-lactic acid) blends. Biomaterials 2005;26(34):6906–15.
[8] Dragunow M. High-content analysis in neuroscience. Nat Rev Neurosci 2008;9(10):779–88.
[9] Mosmann T. Rapid colorimetric assay for cellular growth and survival: application to proliferation and cytotoxicity assays. J Immunol Methods 1983;65(1–2):55–63.
[10] Ishiyama M, Shiga M, Sasamoto K, Mizoguchi M, He PG. A new sulfonated tetrazolium salt that produces a highly water-soluble formazan dye. Chem Pharm Bull 1993;41(6):1118–22.
[11] Simon Jr CG, Khatri CA, Wight SA, Wang FW. Preliminary report on the biocompatibility of a moldable, resorbable, composite bone graft consisting of calcium phosphate cement and poly(lactide-co-glycolide) microspheres. J Orthop Res 2002;20(3):473–82.
[12] Smith PK, Krohn RI, Hermanson GT, Mallia AK, Gartner FH, Provenzano MD, et al. Measurement of protein using bicinchoninic acid. Anal Biochem 1985;150(1):76–85.
[13] Popat KC, Swan EEL, Mukhatyar V, Chatvanichkul KI, Mor GK, Grimes CA, et al. Influence of nanoporous alumina membranes on long-term osteoblast response. Biomaterials 2005;26(22):4516–22.
[14] Singer VL, Jones LJ, Yue ST, Haugland RP. Characterization of PicoGreen reagent and development of a fluorescence-based solution assay for double-stranded DNA quantitation. Anal Biochem 1997;249(2):228–38.
[15] Salinas CN, Anseth KS. The influence of the RGD peptide motif and its contextual presentation in PEG gels on human mesenchymal stem cell viability. J Tissue Eng Regen Med 2008;2(5):296–304.
[16] Muller R, Hahn M, Vogel M, Delling G, Ruegsegger P. Morphometric analysis of noninvasively assessed bone biopsies: comparison of high-resolution computed-tomography and histologic sections. Bone 1996;18(13):215–20.
[17] Barry JJA, Howard D, Shakesheff KM, Howdle SM, Alexander MR. Using a core-sheath distribution of surface chemistry through 3D tissue engineering scaffolds to control cell ingress. Adv Mater 2006;18(11):1406–10.
[18] Ho ST, Hutmacher DW. A comparison of micro CT with other techniques used in the characterization of scaffolds. Biomaterials 2006;27(8):1362–76.
[19] Jones JR, Poologasundarampillai G, Atwood RC, Bernard D, Lee PD. Non-destructive quantitative 3D analysis for the optimization of tissue scaffolds. Biomaterials 2007;28(7):1404–13.
[20] Lin-Gibson S, Cooper JA, Landis FA, Cicerone MT. Systematic investigation of porogen size and content on scaffold morphometric parameters and properties. Biomacromolecules 2007;8(5):1511–8.
[21] Hutmacher DW, Schantz T, Zein I, Ng KW, Teoh SH, Tan KC. Mechanical properties and cell cultural response of polycaprolactone scaffolds designed and fabricated via fused deposition modeling. J Biomed Mater Res 2001;55(2):203–16.
[22] Thomas V, Jagani S, Johnson K, Jose MV, Dean DR, Vohra YK, et al. Electrospun bioactive nanocomposite scaffolds of polycaprolactone and nanohydroxyapatite for bone tissue engineering. J Nanosci Nanotechnol 2006;6(2):1–7.
[23] Sudo H, Kodama HA, Amagai Y, Yamamoto S, Kasai S. In vitro differentiation and calcification in a new clonal osteogenic cell line derived from newborn mouse calvaria. J Cell Biol 1983;96(1):191–6.
[24] Simon Jr CG, Stephens JS, Dorsey SM, Becker ML. Fabrication of combinatorial polymer scaffold libraries. Rev Sci Instrum 2007;78(7):072207.